

Protumoral roles of melanoma inhibitory activity 2 in oral squamous cell carcinoma

Miyako Kurihara^{1,2}, Tadaaki Kirita², Tomonori Sasahira¹, Hitoshi Ohmori¹, Sayako Matsushima¹, Kazuhiko Yamamoto², Anja Katrin Bosserhoff³, Hiroki Kuniyasu¹

¹Department of Molecular Pathology, ²Department of Oral and Maxillofacial Surgery, Nara Medical University, Kashihara, Japan; ³Institute of Pathology, University of Regensburg, Regensburg, Germany

Running title: MIA2 expression in oral cancer

Correspondence to: Hiroki Kuniyasu, M.D., Ph.D., Department of Molecular Pathology, Nara Medical University, 840 Shijo-cho, Kashihara, Nara 634-8521, Japan. E-mail:

cooninh@zb4.so-net.ne.jp

Key words: apoptosis, VEGF, integrin, MAPK

Abbreviation: OSCC; oral squamous cell carcinoma, MIA; melanoma inhibitory activity, VEGF; vascular endothelial growth factor, JNK; c-Jun N-terminal kinase, HNF; hepatocyte nuclear factor, HCC; hepatocellular carcinoma, ITG; integrin, MAPK; mitogen-activated protein kinase, siRNA; small interfering ribonucleic acid, HCR; highly conserved region, PG; prostaglandin

Abstract

The role of melanoma inhibitory activity 2 (MIA2) was examined in human oral squamous cell carcinoma (OSCC). MIA2 expression was observed in 62 (66.7%) of 93 OSCCs and was associated with tumor expansion and nodal metastasis. MIA2 expression was inversely correlated with intratumoral infiltration of lymphocytes. MIA2 expression was found in 3 human OSCC lines. Invasion and anti-apoptotic survival were reduced by MIA2 knockdown in HSC3 cells. The number of MOLT-3 lymphocytes infiltrating the HSC3 cell layer was increased by MIA2 knockdown or MIA2 depletion by MIA2 knockdown and absorption with the antibody. In HSC3 cells, MIA2 knockdown decreased the expressions of vascular endothelial growth factor (VEGF), VEGF-C, VEGF-D. The downregulation of VEGF-C and -D was caused by inhibition of p38 and extracellular signal-regulated kinase (ERK)1/2, respectively. MIA2 was coprecipitated with integrin α 4 and α 5 in HSC3 cells. Integrin α 4 knockdown decreased p38 phosphorylation and increased apoptosis, whereas integrin α 5 knockdown decreased c-Jun N-terminal kinase (JNK) phosphorylation and apoptosis. Inhibition of JNK decreased apoptosis in the HSC3 cells. These findings suggest that the roles of MIA2 might be based on the variety of the integrins and the subtypes of mitogen-activated protein kinase.

Introduction

Oral squamous cell carcinoma (OSCC) is the most common cancer resulting from the oral habits of smoking, reverse smoking, and betel nut chewing, accounting for at least 40% of cancer cases in South Asia, including India and Sri Lanka {Ferlay, 2010 #21}. In Japan, OSCC comprises approximately 1–2% of all cancer morbidity, a rate that is gradually increasing {Matsuda, 2012 #22}. OSCC frequently leads to dysfunction of mastication, speech, and deglutition, which worsen a patient's quality of life. Moreover, the prognosis of OSCC remains poor: the overall 5-year survival rate has remained at approximately 56% over the past 2 decades {Nagler, 2002 #23} {Kademani, 2005 #24}. The poor prognosis of OSCC is associated with local invasion and lymph node metastasis {Lopez-Graniel, 2001 #25}.

Angiogenesis and lymphangiogenesis, pivotal events in tumor progression and metastasis {Adams, 2007 #26} {Avraamides, 2008 #27}, are responsible for local invasion and lymph node metastasis and a subsequently worse prognosis {Miyahara, 2007 #29}. Tumor cells have been reported to induce angiogenesis and lymphangiogenesis by expressing angiogenesis factor vascular endothelial growth factor (VEGF) and the lymphangiogenic factors VEGF-C and VEGF-D {Beck, 1997 #30} {Yonemura, 1999 #32} {Tsurusaki, 1999 #33}. In OSCC, like in other tumors, VEGF predominantly induces tumor angiogenesis, whereas VEGF-C and VEGF-D induce lymphangiogenesis {Shintani, 2004 #34}. A significant association between elevated VEGF circulating levels and clinical stage {Shang, 2002 #35} and a possible relationship between the VEGF-C and/or VEGF-D expression levels and the development of lymphatic tumor spread were revealed in patients with OSCC {Shintani, 2004 #34}. We previously reported that melanoma inhibitory activity (MIA) is closely involved in tumor progression and nodal metastasis by the increments of VEGF-C and VEGF-D in OSCC {Sasahira, 2010 #2}.

MIA2 belongs to the MIA gene family, which contains MIA, OTOR, and Tango

{Bosserhoff, 2002 #70}. MIA2 is mapped to the gene locus of human chromosome 14q13 {Bosserhoff, 2003 #44}. MIA and OTOR are exclusively expressed in the cartilage and cochlea, respectively, whereas MIA2 is expressed exclusively in the liver {Bosserhoff, 2003 #44}. MIA2 expression is transcriptionally regulated by the hepatocyte nuclear factor (HNF)-1 binding site {Hellerbrand, 2005 #62}. MIA2 is expressed in hepatocellular carcinoma (HCC) but not in bladder, breast, or prostate cancer {Hellerbrand, 2005 #62}. MIA2 inhibits HCC growth and invasion and consequently acts as a tumor suppressor {Hellerbrand, 2008 #53}. Hepatic MIA2 expression is increased in patients with liver fibrosis or cirrhosis and tumor growth factor- β (TGF- β)-induced MIA2 expression in hepatocytes {Bosserhoff, 2003 #90}. It is well known that TGF- β signaling is deranged in HCC {Hellerbrand, 2008 #53}. Therefore, it may be speculated that TGF- β signaling contributes to the reduced MIA2 transcriptional activity observed in HCC. Loss of HNF-1 expression in HCC affects tumorigenicity by downregulating MIA2 {Hellerbrand, 2008 #53}. In OSCC, the expression and role of MIA2 have not been elucidated previously.

In this study, we investigated the relationship between MIA2 expression and clinicopathological characteristics to determine its functional role in OSCC.

Material and Methods

Patients and tumor specimens

Ninety-three formalin-fixed (43 men, 50 women) paraffin-embedded specimens of primary OSCC cases were randomly selected, which were operated at Nara Medical University Hospital from 2002 to 2005. Medical records and prognostic follow-up data were obtained from the patient database administered by the hospital. The primary site of the cases was tongue (52 cases), gingiva (27 cases), buccal mucosa (9 cases) and other (5 case). The tumors were classified according to the International Union Against Cancer TNM classification system {Kreppel, 2010 #78}.

Immunohistochemistry

Consecutive 3 μm sections were cut from each block. Immunohistochemistry was performed by the immunoperoxidase technique, following antigen retrieval by incubation with pepsin (Sigma Chemical, St. Louis, MO) for 20 min, specimens were rinsed with phosphate-buffered saline (PBS, Sigma). Anti-MIA2 antibody (Abcam, Cambridge, UK) diluted at 0.5 $\mu\text{g}/\text{ml}$ was used for primary antibody. After overnight incubation at room temperature, specimens were rinsed with PBS and incubated at room temperature for 1 h with secondary antibody conjugated to peroxidase (0.2 $\mu\text{g}/\text{ml}$). The specimens were then rinsed with PBS and color-developed with diaminobenzidine (DAB) solution (DAKO, Carpinteria, CA). After washing, specimens were counterstained with Meyer's hematoxyline (Sigma). Immunostaining of all samples was performed at the same conditions of antibody reaction and DAB exposure.

Evaluation of immunohistochemistry

The intensity of immunoreactivity for MIA2 was classified with 4 grades; grade 0 was no

immunoreactivity, grade 1 was weak, grade 2 was moderate, and grade 3 was strong immunoreactivity (Fig. 1c-f). Cases with grade 2 - 3 immunoreactivity were judged as positive for MIA2 expression. Infiltration pattern of lymphocytes was classified in 3 patterns (Fig. 3). Grade A is the scattered infiltration of lymphocytes at only the outside of tumor nests. Grade B is intermediate infiltration of lymphocytes at the outside and inside of tumor nests. Grade C is marked infiltration of lymphocytes at the outside and inside of tumor nests.

Cell lines and cell culture

HSC3 (derived from metastatic focus of human tongue SCC), HSC4 (derived from primary tumor of the same case of HSC3), and KON (derived from nodal metastatic focus of human oral floor cell lines) were purchased from Health Science Research Resources Bank (Osaka, Japan). MOLT-3 T-lymphoblastic leukemia cell line was purchased from Dainihon Pharmaceutical, Tokyo, Japan. Cells were maintained in Dulbecco's modified Eagle's medium (DMEM) (Wako Pure Chemical, Osaka, Japan) supplemented with 10% FBS (Sigma) in 5% CO₂ and 95% air at 37°C. For MIA2 inhibition, antibody to MIA2 (Abcam, 1 µg/ml) was added to culture medium and cultured for 48 h. For the control, rabbit serum (DAKO, 1 µg/ml) was used. Extracellular signal-regulated kinase (ERK) inhibitor (Calbiochem-Novabiochem, Darmstadt, Germany), p38 mitogen-activated protein kinase (MAPK) inhibitor (SB239063, Sigma), and JNK inhibitor (SP600125, Biomol, Hamburg, Germany) were treated for 24 h. Apoptosis was assessed by staining with Hoechst33258 fluorescent dye (Wako). Number of apoptotic cells was counted by observation of 500 cells.

Coculture of OSCC cell with T lymphocytes

HSC3 cells and (5×10^2) and MOLT-4 cells (5×10^2) were seeded and cultured for 24 h in 96-well

culture dish. Cells fixed with 4% paraformaldehyde for 6 h at 4°C were treated with peroxidase-conjugated anti-CD3 antibody (DAKO, 0.5 µg/ml) for 30 min at 37°C. Cells were treated with tetramethylbenzidine (DAKO) after rinse with PBS for color development. The reaction was stopped with 0.2N H₂SO₄ and the color concentration was measured at O. D. 450 nm. Anti-MIA2 antibody (Abcam) was used for antibody treatment with a concentration of 0.5 µg/ml.

Short interferent RNA

Stealth Select RNAi (siRNA) for *MIA*, *MIA2*, *ITGA4*, *ITGA5* and Negative siRNA (control siRNA) were purchased from Invitrogen (Carlsbad, CA). siRNAs (20 nM) were transfected with Lipofectamine2000 (Invitrogen) according to the manufacture's recommendations. Effect of siRNA was confirmed by real-time RT-PCR.

Transwell infiltration assay of T lymphocytes

Our previous method was modified {Kuniyasu, 2004 #81}. HSC3 cells (1×10^4) were seeded on the bottom of the insert well coated with fibronectin (pore size 3 µm; diameter 5 mm, Becton-Dickinson, Bedford, MA), which was set on the well and exchanged medium to DMEM with 2% bovine serum albumin (BSA; Sigma). MOLT-3 cells (5×10^3), which were surface-labeled with PKH26 chemifluorescent dye (Zynaxis, Malvern, PA) were seeded on each insert using 2% BSA-DMEM. After 6 h incubation, infiltrating MOLT-3 cells were counted by fluorescence-positive cells in the lower chamber were counted by an autocytofluorometer (Sysmecs, Kobe, Japan).

Quantitative reverse transcription-polymerase chain reaction

The extraction of total RNA was carried out using RNeasy Mini Kit (Qiagen Genomics, Bothell, WA) and total RNA (1 µg) was synthesized with the ReverTra Ace- α -RT Kit (Toyobo, Osaka, Japan). Quantitative reverse transcription-polymerase chain reaction (qRT-PCR) was performed by StepOne Real-Time PCR Systems (Applied Biosystems, Foster City, CA) using Fast SYBR Green Master Mix (Applied) and analyzed the relative standard curve quantification method {Livak, 2001 #79}. PCR condition was set according to the provider's instructions. ACTB mRNA was amplified for internal control (GenBank accession No. NM 001101). Each amplification reaction was evaluated by a melting curve analysis. For visualizing PCR products, agarose gel electrophoresis was performed with ethidium bromide staining.

Preparation of conditioned medium

HSC3 cells were cultured in 2% BSA-DMEM for 12 hours in treatment with MIA2 siRNA or anti-MIA2 antibody (Abcam, 0.5 µg/ml). Then the conditioned medium was filtered with 0.2 µm-filter (Becton-Dickinson Labware).

Immunoblotting

Cell lysate was extracted as previously described {Kuniyasu, 2002 #95}. Cell lysate (50 µg) was separated by 12.5% SDS-PAGE. Proteins were blotted onto nitrocellulose membrane electronically. The membrane was treated with primary antibodies to MIA and MIA2 (Abcam), integrin α 4, integrin α 5, phosphorylated ERK1/2, phosphorylated JNK, phosphorylated p38, VEGF, VEGF-C, VEGF-D (Santa-Cruz Biotechnology, Santa-Cruz, CA). An α -tubulin antibody was used to assess the levels of protein loaded per lane (Oncogene Research Products, Cambridge, MA). The immune complex was visualized with an ECL Western-blot detection system (Amersham, Aylesbury, UK).

Immunoprecipitation

Immunoprecipitation was performed according to the method described previously {Kuniyasu, 2001 #96}. The lysates were pre-cleaned in lysis buffer with protein A/G agarose (Santa Cruz) for 1 h at 4°C and subsequently centrifuged. The supernatants were incubated with precipitation antibody and protein A/G agarose for 3 hours at 4°C. Precipitates were collected by centrifugation and washed 5 times with lysis buffer. Precipitates solubilized with sample buffer (Sigma, 40 µg) were subjected to immunoblot analysis. For precipitation, antibodies to integrin $\alpha 4$, integrin $\alpha 5$ (Santa-Cruz) were used. For detection, antibodies to MIA and MIA2 (Abcam) were used.

Statistical analysis

Statistical analysis of experimental data was done by Mann-Whitney U test and chi-square test. Statistical significance was defined as a two-sided *P* value of less than 0.05.

Results

Relationship between MIA2 expression and clinical parameters

MIA2 expression was examined by immunohistochemistry in 93 cases of OSCC (Table 1). MIA2 immunoreactivity was detected in the cytoplasm of hepatocytes and cancer cells of OSCC (Figs. 1a, c–f). In contrast, HCC cells did not show MIA2 immunoreactivity (Fig. 1b). Cases with grade 2 or 3 immunoreactivity were judged positive for MIA2 expression.

MIA2 expression was observed in 62 (66.7%) of the 93 cases and was associated with T classification (tumor expansion) and nodal metastasis. Of the 22 cases of local invasion (T3 or T4), 14 (63.6%) expressed MIA2, whereas only 18 (25.3%) of the 71 cases of early cancer (T1 or T2) expressed MIA2 ($P = 0.0017$). Of the 30 cases with nodal metastasis (n+), 17 (56.7%) showed MIA2 expression, whereas only 15 (23.8%) of the 63 cases without nodal metastasis (n–) expressed MIA2 ($P = 0.0025$). However, no significant relationship was found between MIA2 grading and the other parameters including age, sex, primary site, clinical stage, histological differentiation, and tumor recurrence.

MIA2 expression in OSCC cell lines

We compared the MIA2 expression in HSC-3 (high metastatic cell line), HSC4 (low metastatic cell line), and KON (metastatic lymph nodes cell line) using qRT-PCR and immunoblotting (Fig. 2a, b). The MIA2 expression level was higher in HSC3 than those in HSC-4 and KON. The MIA2 expression in OSCC cells was compared with the MIA expression. The MIA2 and MIA were expressed in all OSCC cell lines at various levels.

Effect of MIA2 knockdown in the OSCC cell lines

We next performed MIA2 knockdown by siRNA treatment to examine the roles of MIA2 on cell

growth, invasion, and apoptosis in HSC3 cells (Figs. 2c–f). MIA2 siRNA treatment decreased mRNA and protein in HSC3 cells (Fig. 2c). Compared with the control siRNA treatment, cell invasion and anti-apoptotic survival were reduced by MIA2 siRNA treatment ($P = 0.0417$ and $P = 0.018$, respectively). Cell growth with MIA2 siRNA treatment was not significantly different from that before the treatment.

MIA2 expression and lymphocyte infiltration

The infiltration pattern of the lymphocytes was classified into 3 patterns (Fig. 3). Grade C showed the most pronounced lymphocyte infiltration among the 3 patterns, whereas grade A showed mild and remote lymphocytes infiltration. As shown in Table 2, MIA2 expression was inversely associated with lymphocyte infiltration. Of the 31 grade A cases, 17 (54.8%) showed MIA2 expression, whereas only 4 (12.9%) of the 31 grade C cases expressed MIA2. This result suggests that MIA2 might inhibit intratumoral lymphocyte infiltration.

HSC3 cells and MOLT-3 lymphocytes were cocultured to confirm the lymphocyte inhibitory effect of MIA2 (Fig. 4a). The number of MOLT-3 cells was not affected by the coculturing. Next, we conducted a trans-cell layer assay using an insert chamber (Fig. 4c–e). The MIA2 protein levels in the cultured medium of HSC3 cell was examined (Fig. 4c). MIA2 knockdown and absorption by anti-MIA2 antibody depleted MIA2 protein in the medium. The number of MOLT-3 lymphocytes that passed through the HSC3 cell layer at the bottom of the insert was then counted. The infiltrating cell number was increased by MIA2 depletion by MIA2 knockdown and the antibody treatment.

Effect of MIA2 knockdown on the VEGF, VEGF-C, and VEGF-D expressions in the HSC3 OSCC cells

MIA is a known angiogenic and lymphangiogenic factor inducing VEGF and VEGF-D {Sasahira, 2008 #4} {Sasahira, 2010 #2}. As such, we examined the effect of MIA2 knockdown on the levels of mRNA and protein of VEGF, VEGF-C, and VEGF-D and compared it with the effect of MIA knockdown in HSC3 cells. Treatment with specific siRNAs to MIA2 or MIA decreased the levels of mRNA and protein in the HSC3 cells (Figs. 5a, b). The HSC3 cells after MIA2 knockdown showed modestly inhibited VEGF and VEGF-C expressions compared with those after MIA knockdown (Figs. 5c, d). In contrast, the HSC3 cells after MIA2 knockdown showed VEGF-D downregulation similar to that in cells after MIA knockdown (Fig. 5e). It is interesting that the double knockdown of MIA2 and MIA showed less of an inhibitory effect on VEGF and VEGF-C downregulation, whereas it showed a greater inhibitory effect on VEGF-D downregulation (Figs. 5c–e). Finally, the HSC3 cells after MIA or MIA2 knockdown were treated with ERK1/2 and p38 inhibitors (Fig. 5f). In both MIA and MIA2 knockdown, VEGF-C expression was decreased by p38 inhibition, whereas VEGF-D was decreased by ERK1/2 inhibition.

Comparison of the role of integrins in MIA2 function

MIA is a known interacting partner of integrins $\alpha 4$ and $\alpha 5$ {Bauer, 2006 #295}. As such, we examined the physical association between MIA2 and the integrins (Fig. 6a). The HSC3 lysates showed coprecipitation between MIA2 and integrin $\alpha 4$ or $\alpha 5$ as with MIA. MIA2 showed higher affinity with integrin $\alpha 4$ than that with integrin $\alpha 5$ unlike MIA in the HSC3 cells. Knockdown of the expression of integrins $\alpha 4$ (*ITGA4*) and $\alpha 5$ (*ITGA5*) was confirmed in the HSC3 cells (Fig. 1b). Using the knockdown system, the phosphorylation status of the mitogen-activated protein kinase (MAPK) family was examined (Fig. 6c–e). In the MIA-knockdown HSC3 cells, which expressed *MIA2*, *ITGA4* knockdown decreased p38 phosphorylation. In contrast, *ITGA5*

knockdown decreased phosphorylation of p38 and JNK. In MIA2-knockdown HSC3 cells expressing *MIA*, knockdown of *ITGA4* and *ITGA5* decreased phosphorylation of p38 and JNK.

Finally, we examined the effect of *ITGA4* or *ITGA5* knockdown and MAPK inhibitors on apoptosis in MIA-knockdown HSC3 cells (Fig. 6f, g). *ITGA4* knockdown increased apoptosis, whereas *ITGA5* knockdown decreased apoptosis. The inhibition of JNK decreased apoptosis, whereas inhibition of p38 increased apoptosis. These findings suggest that JNK activation by MIA2 through integrin $\alpha 5$ might induce apoptosis. In contrast, p38 activation through integrin $\alpha 4$ and $\alpha 5$ might suppress apoptosis.

Discussion

MIA2 is isolated as a second member of the MIA homologous gene family. MIA is a protumoral factor in the progression and metastasis of malignant melanoma and OSCC. In contrast, MIA2 is downregulated in HCC, which suggests that MIA2 has a putative tumor suppressive function. It is interesting that our data on OSCC suggest that MIA2 might act as a protumoral factor similar to MIA.

In clinical study, MIA2 expression was associated with tumor expansion, nodal metastasis, less lymphocyte infiltration, and advanced-stage OSCC. Highly metastatic OSCC cell lines expressed MIA2 at higher levels than a low metastatic cell line. MIA2 knockdown was associated with inhibition of cell invasion, anti-apoptotic survival, and VEGF, VEGF-C, and VEGF-D expressions. These results suggest that MIA2 increases invasion, survival, and angiogenesis and inhibits host anticancer immunity.

MIA2 shares protein homology, including *src* homology domain-3, with MIA {Bosserhoff, 2004 #67}. The immunoprecipitation assay in the present study showed that MIA2 and MIA bound to integrins $\alpha 4$ and $\alpha 5$; however, MIA2 showed higher affinity to integrin $\alpha 4$ than to integrin $\alpha 5$. MIA activated p38 and JNK through integrins $\alpha 4$ and $\alpha 5$, whereas MIA2 activated p38 through integrin $\alpha 4$ and $\alpha 5$, and activated JNK through integrin $\alpha 5$. Moreover, the MIA2-integrin $\alpha 5$ -JNK signal increased apoptosis, whereas the MIA2-integrin $\alpha 4$ -p38 signal decreased apoptosis.

MIA2 played a pro-angiogenic role by increasing VEGF family expression. The increment was modest compared with that by MIA; however, MIA2 showed a less pronounced increase in VEGD and VEGF-C than that by MIA. In contrast, VEGF-D upregulation by MIA2 was at the same level to that by MIA. The VEGF-C upregulation signal by MIA2 was carried through p38, which is also associated with MIA-induced VEGF family upregulation {Sasahira,

2008 #4} {Sasahira, 2010 #2}. In contrast, the VEGF-D upregulation signal by MIA2 was carried through ERK1/2 as found in that by MIA {Sasahira, 2008 #113}. Co-expressed MIA and MIA2 was found in most OSCC cell lines and human OSCC tumors, and expression of the VEGF family might be affected by MIA and MIA2 by a synergic (as show in VEGF-D) or nonsynergic (as shown in VEGF and VEGF-C) manner.

MIA2 expression was inversely associated with lymphocyte infiltration into the tumors. MIA binds to integrin $\alpha 4$, which is expressed in the host immune cells and suppresses lymphokine-activated killer cell cytotoxicity {Jachimczak, 2005 #40}. Our data showed that MIA2 also bound to integrin $\alpha 4$, which might inhibit lymphocyte infiltration into the tumor. The coculture of HSC3 cells and MOLT-3 lymphocytes did not induce cell death in MOLT-3 cells, an observation suggesting that MIA2 possesses no cytotoxic effect on lymphocytes. Since MIA binds to fibronectin to induce tumor cell detachment from the extracellular matrix {Bosserhoff, 2003 #44}, MIA2 might also bind to fibronectin. Fibronectin induces chemotaxis of T lymphocytes in combination with stromal cell-derived factor 1 α {Savino, 2002 #94}. The masking of fibronectin by MIA or MIA2 might inhibit chemotaxis of the T lymphocytes.

MIA is regulated by HMGB1 via a highly conserved region promoter element in the 5'-flanking region of the *MIA* gene {Poser, 2003 #37}. We reported previously that HMGB1 affected MIA expression in OSCC cells {Sasahira, 2008 #4}. Comparison of MIA and MIA2 protein levels showed no association between them. Therefore, MIA2 might not be regulated by HMGB1. In the liver, MIA2 expression is transcriptionally regulated by hepatic nuclear factor (HNF)-1 {Bosserhoff, 2003 #90} {Bosserhoff, 2004 #67} {Hellerbrand, 2008 #53}. HNF-1A expression is reported in human OSCC {O'Donnell, 2005 #84}, suggesting that it induces MIA2 expression in OSCC. Prostaglandin E2 (PGE2) activates T-cell factor (same as HNF)-dependent transcription {Shao, 2005 #87}. PGE2 is highly involved in tumor growth in head and neck

cancers {Abraham, 2010 #88}. Therefore, MIA2 might be a common tumor-associated factor in OSCC.

MIA2 is expressed at high levels and acts as an antitumor factor in the liver {Bosserhoff, 2004 #67} {Hellerbrand, 2005 #62} {Hellerbrand, 2008 #53}. MIA2 expression is repressed in hepatitis, cirrhosis, and hepatoma, which is associated with cell proliferation {Hellerbrand, 2008 #53} {Xu, 2011 #89}. In contrast, MIA2 acts as a protumoral factor in OSCC. MIA2 affinity to the MIA receptors, integrins $\alpha 4$ and $\alpha 5$, suggests that MIA2 might act as a competitive inhibitor of MIA. Otherwise, HCC cells express integrin $\alpha 4$ at a markedly lower level than that of integrin $\alpha 5$ {Fu, 2010 #93}. These features in the liver suggest that MIA2 might act as a pro-apoptotic factor through integrin $\alpha 5$. Moreover, OSCC concurrently expressed MIA2 with MIA at high frequency (80%, data not shown). The overlapping of signals from MIA2 and MIA through integrin $\alpha 4$ and $\alpha 5$ might result a protumoral role in OSCC. MIA is expressed in the liver at low levels {Su, 2002 #92}. A lack of synergism between MIA and MIA2 also might emphasize a pro-apoptotic role in the liver.

These data suggest that MIA2 might act as a protumoral factor that was influenced by concurrent expression of MIA, receptor integrin expression patterns, and activation pattern of MAPK family in OSCC. The frequent expression in OSCC suggests that MIA2 is a relevant target for cancer treatment.

Table 1. Correlation between melanoma inhibitory activity 2 (MIA2) expression and clinicopathological characteristics of human oral squamous cell carcinoma

Parameters		MIA2 expression grade		<i>P</i> value ¹⁾
		0–1	2–3	
Age	<60	17	9	NS
	>60	44	23	
Sex	Male	27	16	NS
	Female	34	16	
Site	Tongue	35	17	NS
	Gingiva	16	11	
	Buccal mucosa	6	3	
	Other	4	1	
Differentiation ²⁾	Well	37	25	NS
	Mod	22	7	
	Poor	2	0	
T factor ³⁾	T1, T2	53	18	0.0010
	T3, T4	8	14	
Nodal metastasis	(–)	48	15	0.0019
	(+)	13	17	
Pathologic stage ³⁾	I, II	41	17	NS
	III, IV	20	15	
Recurrence	(–)	32	16	NS
	(+)	20	12	

¹⁾Fisher exact *t* test. ²⁾Histological differentiation: Well, well-differentiated; Mod, moderately differentiated; Poor, poorly differentiated. ³⁾According to the tumor, node, metastasis classification.

Table 2. Relationship between melanoma inhibitory activity 2 (MIA2) expression and infiltration pattern of lymphocytes in oral squamous cell carcinoma

Lymphocyte infiltration pattern	MIA2 expression	
	Grade 0–1	Grade 2–3
Grade A	14 (23%)	17 (53%)
Grade B	20 (33%)	11 (34%)
Grade C	27 (44%)	4 (13%)

$P = 0.00248$ (χ^2 test)

Figure legends**Figure 1. Expression of melanoma inhibitory activity 2 (MIA2) in oral squamous cell carcinoma (OSCC)**

(a) MIA2 immunoreactivity in a non-tumorous, non-hepatitis liver specimen that was used as a positive control. The cytoplasm of the hepatocytes in an acute hepatitis case showed high-grade MIA2 immunoreactivity. (b). A specimen of human hepatocellular carcinoma was examined as a negative control. It showed no MIA2 immunoreactivity. (c–f) Immunohistochemical analysis of MIA2 expression in OSCC cases. Positive immunoreactivity was seen in the cytoplasm of the cancer cells. (c) A well-differentiated stage I OSCC case (T1 N0 M0) showed no MIA2 immunoreactivity (grade 0). (d) A well-differentiated stage II OSCC case (T2 N0 M0) showed weak MIA2 immunoreactivity (grade 1). (e) A well-differentiated stage IV OSCC case (T4 N0 M0) showed moderate MIA2 immunoreactivity (grade 2). (f) A well-differentiated stage III OSCC case (T3 N1 M0) showed strong MIA2 immunoreactivity (grade 3). Bar, 50 μ m.

Figure 2. Melanoma inhibitory activity 2 (MIA2) expression and roles in oral squamous cell carcinoma (OSCC) cell lines.

(a, b) MIA2 and MIA mRNA expressions were examined using qRT-PCR (a) and immunoblotting (b) in the highly metastatic cell line HSC3, low metastatic cell line HSC4, KON cell line derived from metastatic lymph nodes cells. The tissues of non-tumorous, non-hepatitis liver and hepatocellular carcinoma were examined as positive and negative control, respectively for MIA2 expression. MIA expression was also examined. β -Actin served as the loading control. (c) The effect of MIA2 siRNA treatment on MIA2 mRNA expression in HSC3 cells. MIA2 protein levels were also shown in the inset. The effects of MIA2 knockdown on cell growth (d), invasion (e), and apoptosis (f) in the HSC3 cells. Error bar; SD.

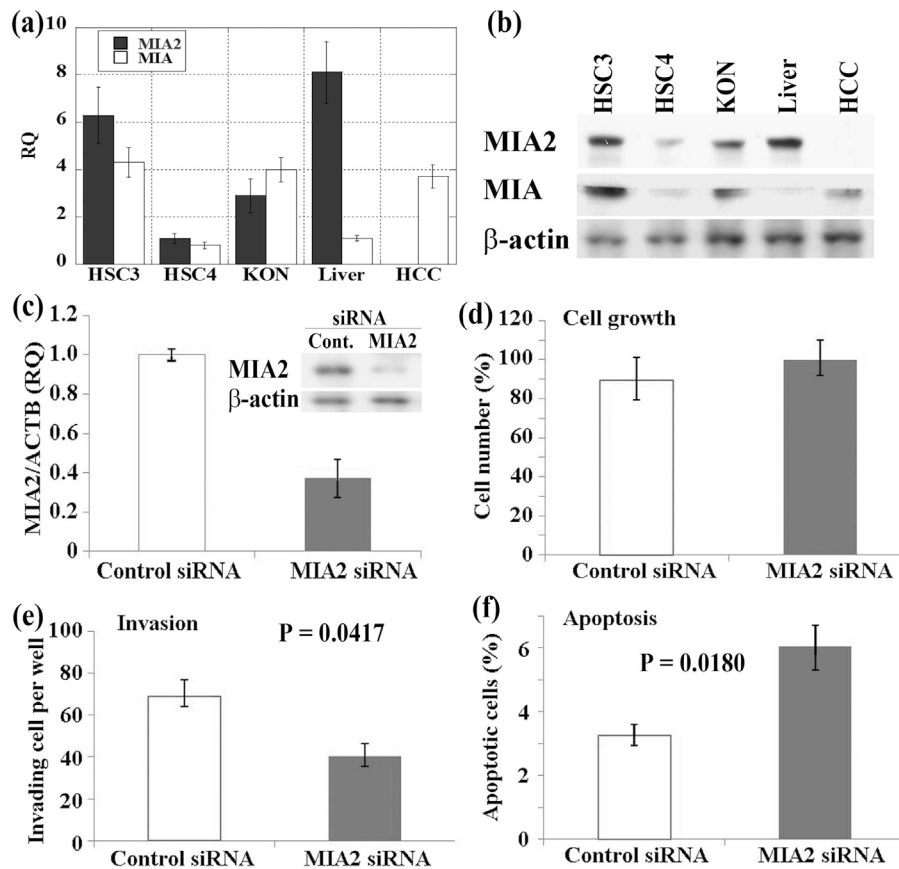


Figure 3. Infiltration pattern of lymphocytes in oral squamous cell carcinoma (OSCC)

The infiltration pattern of lymphocytes in OSCC was classified into 3 patterns: grade A, scattered infiltration of lymphocytes at only the outside of the tumor nests; grade B, intermediate infiltration of lymphocytes at the outside and inside of tumor nests; grade C, marked infiltration of lymphocytes at the outside and inside of the tumor nests. Bar, 100 μ m.

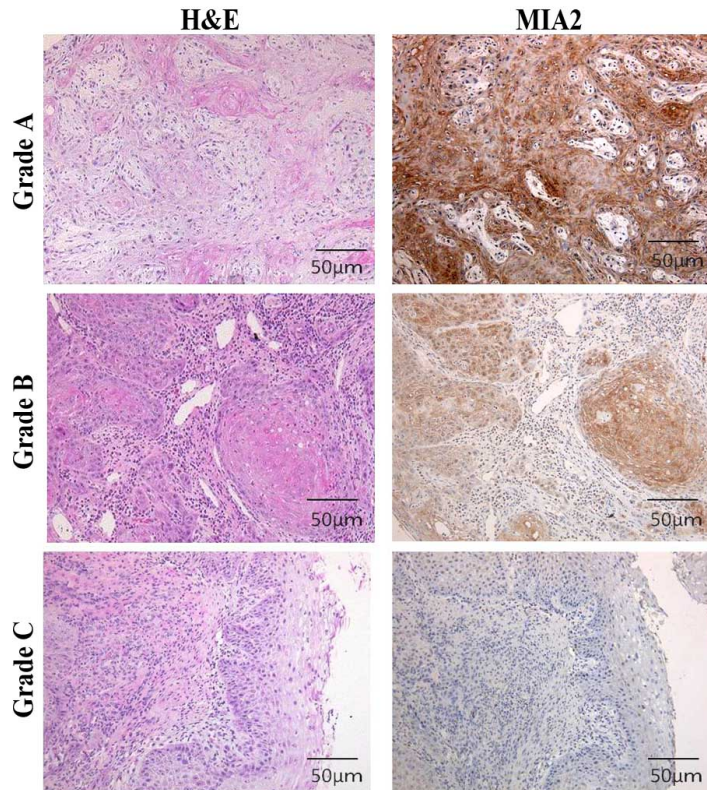


Figure 4. Transwell infiltration of MOLT-3 lymphocytes through an HSC3 cell layer

(a) The HSC3 and MOLT-3 cells were cocultured with melanoma inhibitory activity 2 (MIA2) siRNA or control siRNA. (c, d) Inhibition of transwell infiltration of MOLT-3 cells. The number of MOLT-3 cells infiltrating through the HSC3 cell layer at the bottom of the insert was compared with that using the insert without cell layer. (c) The cells were exposed to MIA2 siRNA or control siRNA. (d) The cells were treated with control serum or anti-MIA2 antibody. Error bar; SD.

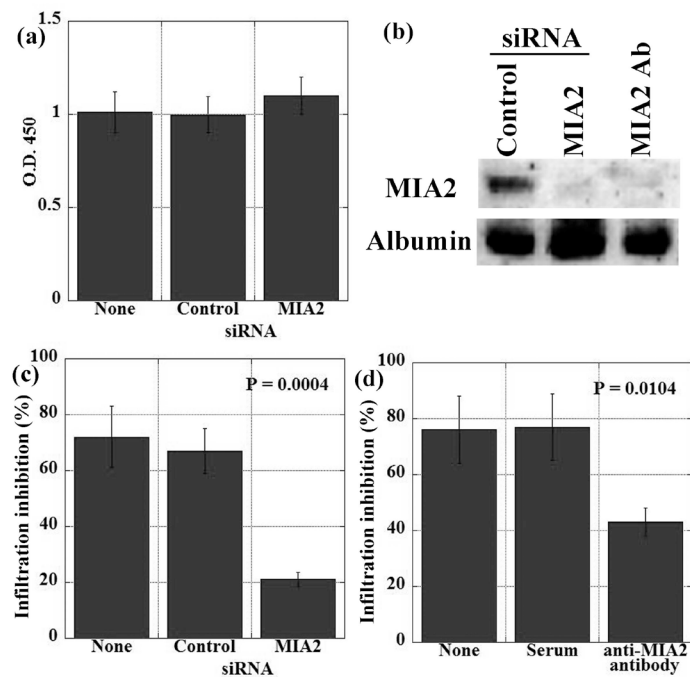


Figure 5. Effect of knockdown of melanoma inhibitory activity 2 (MIA2) and/or MIA on vascular endothelial growth factor (VEGF), VEGF-C, and VEGF-D expressions in the HSC3 cells

Knockdown of MIA (a) and/or MIA2 (b) was confirmed using qRT-PCR and immunoblotting. The expressions of VEGF (c), VEGF-C (d), and VEGF-D (e) were examined by qRT-PCR and immunoblotting in HSC3 cells with knockdown of MIA, MIA2, or MIA+MIA2. (f) Expression of VEGF-C and -D was examined using qRT-PCR and immunoblotting in MIA or MIA2 knockdown HSC3 cells treated with inhibitors of ERK1/2 (ERK-I) or p38 (p38-I). Error bar; SD.

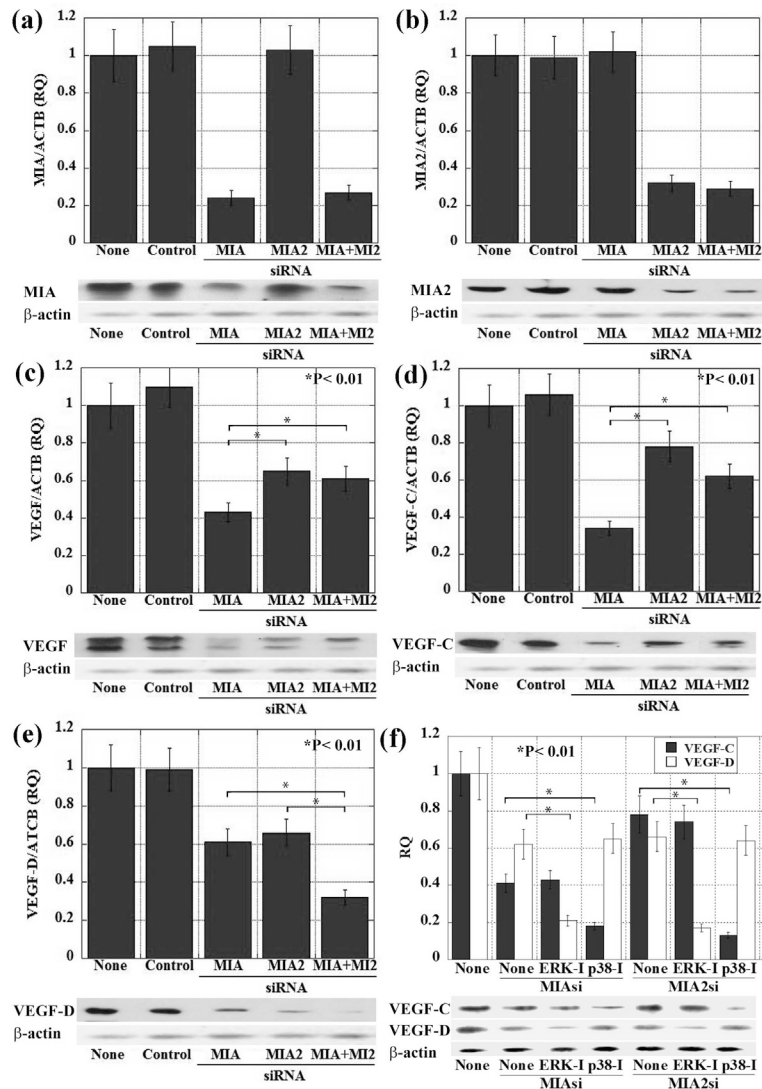


Figure 6. Roles of integrin and mitogen-activated protein kinase (MAPK) in melanoma inhibitory activity 2 (MIA2) function

(a) Immunoprecipitation of the HSC3 cell lysate precipitated with antibodies to integrin $\alpha 4$ (Itg $\alpha 4$) or integrin $\alpha 5$ (Itg $\alpha 5$), detected with antibodies to MIA or MIA2. Precipitation and detection by IgG was done for negative control. Coomassie blue staining of slot blot samples was served as a control for protein content. (b) Knockdown of integrin $\alpha 4$ (*ITGA4*) or integrin $\alpha 5$ (*ITGA5*) was examined using qRT-PCR and immunoblotting. (c) Phosphorylation levels of MAPK families were examined by immunoblotting in HSC3 cells with concurrent knockdown of MIA or MIA2 and *ITGA4* or *ITGA5*. (d, e) Phosphorylation levels of the MAPK families were semiquantified with standardization to those in HSC3 cells untreated with siRNA. (f, g) Effect of knockdown of *ITGA4* or *ITGA5*, p38 inhibitor (p38-I), or JNK (JNK-I) on trichostatin A-induced apoptosis. Percentage of apoptotic cells to 500 counted cells was calculated. Error bar; SD.

